Peer-reviewed version available at *Proteomes* **2018**, *6*, 52; doi:10.3390/proteomes6040052

1 **Title:** *Actinobaculum massiliense* proteome profiled in polymicrobial urethral catheter biofilms

2 **Running Title:** *Actinobaculum massiliense* in polymicrobial catheter biofilms

3

4 Yanbao Yu[a], Tamara Tsitrin[a], Harinder Singh[a], Sebastian Doerfert[b*], Maria Sizova[b^], Slava Epstein[b]
5 and Rembert Pieper[a#]

6

7 [a] J. Craig Venter Institute, 9605 Medical Center Drive, Rockville, Maryland 20850

8 [b] Northeastern University, 360 Huntington Avenue, Boston, MA 02115

9

10 [#]Corresponding author: Rembert Pieper, Email: rpieper@jcvi.org; Tel: (301) 795-7605.

11 *current affiliations: The University of Huntsville in Alabama, Huntsville, AL 35899; ^Evelo Biosciences,
12 Cambridge, MA 02139

13

14 ## Abstract

15 *Actinobaculum massiliense*, a Gram-positive anaerobic coccoid rod colonizing the human urinary
16 tract, belongs to the taxonomic class of Actinobacteria. We identified *A. massiliense* as a cohabitant
17 of urethral catheter biofilms (CB). The CBs also harbored common uropathogens such as *Proteus*
18 *mirabilis* and *Aerococcus urinae*, supporting the notion that *A. massiliense* is adapted to a life style
19 in polymicrobial biofilms. We isolated a strain from an agar colony derived from a clinical sample.
20 Using 16S rRNA gene sequencing and shotgun proteomics, we identified and characterized *A.*
21 *massiliense*, comparing the isolate grown *in vitro* and four clinical '*in vivo*' samples. Based on

abundances of proteins in the *in vivo* milieu, we assessed their functions related to nutrient import and responses to hostile host conditions characterized by neutrophil infiltration. Two putative subtilisin-like proteases and a heme/oligopeptide transporter were highly expressed *in vivo* and are perhaps important for survival in the host milieu. The uptake of xylose/glucuronate and oligopeptides apparently enables feeding metabolites into mixed acid fermentation and peptidolysis pathways, respectively, to generate energy. A putative polyketide synthase which may generate a secondary metabolite interacting with either the host or co-colonizing microbes was identified. The enzyme may contribute to *A. massiliense* persistence in CBs.

Introduction

Actinobaculum massiliense is a Gram-positive, facultatively anaerobic coccoid rod and apparently rare pathogen that is able to infect the human urinary tract [1]. A case report described the species as the cause of catheter-associated recurrent cystitis in an elderly female patient and resistance to the antibiotics trimethoprim/sulfamethoxazole and rifamycin while sensitive to doxycycline [1]. A different report associated *A. massiliense* with urosepsis [2]. The bacterium is taxonomically part of the order Actinomycetales and class Actinobacteria. Twenty years ago, the genus *Actinobaculum* was distinguished from Actinomycetes and Arcanobacteria by Lawson *et al.* based on 16S rRNA gene sequence comparisons [3]. Evaluating the literature, the most common opportunistic pathogen of this genus is *Actinobaculum schaalii* which has been associated with urinary tract infections (UTI), catheter-associated UTIs (CAUTI), abscesses, urosepsis and bacteremia [4,5]. Due to its fastidious growth under aerobic conditions and morphological similarity to commensal urogenital organisms, *A. schaalii* may be a more frequent cause of UTI, asymptomatic bacteriuria (ASB) and CAUTI than current epidemiological data suggest [4]. By interpreting 16S rRNA and DNA hybridization data, *Actinobaculum spp.* were reclassified as *Actinotignum spp.,* including *Actinotignum schaalii* [6]. Data for *A. massiliense* strains, deposited as strains CCUG 47753(T) and DSM 19118(T), suggest that

Peer-reviewed version available at *Proteomes* **2018**, *6*, 52; doi:10.3390/proteomes6040052

some strains belong to the species *A. schaalii* while others represent a new species termed *Actinotignum sanguinis* [6]. Given the uncertainty of *A. massiliense* strain assignments to a genus, we use the original taxon, *Actinobaculum massiliense*, in the context of this report. In addition to 16S rRNA analyses, mass spectrometry-based microbial identification methods such as MALDI-TOF were introduced to allow more frequent identification of *Actinotignum/Actinobaculum spp.* from clinical urine isolates [7].

The growth of *Actinotignum/Actinobaculum spp.* in an aerobic milieu on blood agar *in vitro* has been successful occasionally. Anaerobic culture appears to result in improved recovery rates in the form of small, gray colonies on blood agar plates [5]. The complete genome sequence of the *A. schaalii* strain CCUG 27420 was published in 2014 [8]. Draft genome sequences of *A. massiliae* (*massiliense*) - strains FC3 [9] and ACS-171-V-COL2 - submitted to the EMBL/GenBank/DDBJ databases in 2012 [10] were reported. Reference proteomes with 1444 protein sequences (*A. schaalii*; No. UP000035032) and 1696 sequences (*A. massiliense*; No. UP000009888) are deposited in the UniProt Proteome database. The genome analyses of *A. schaalii* CCUG 27420 and *A. massiliense* FC3 revealed genes for fimbriae and capsule formation [8] and for bacteriocin and toxin-antitoxin systems [9], respectively. The data suggest that *A. massiliense* has acquired more genes via lateral gene transfer than *A. schaalii*, while the species also share several putative virulence factors [9]. While clinical strains have been linked to a few CAUTI cases, the persistence of *Actinotignum/Actinobaculum spp.* on the catheter surface, as polymicrobial biofilm residents, has not been studied to date. To our knowledge, little is known about their metabolic adaptation to the human urinary tract and urinary nutrient resources. The goal of this investigation was to characterize *A. massiliense* isolates residing in urethral polymicrobial CBs with respect to energy metabolism, expression of potential virulence and fitness factors and the microbial-host immune cell crosstalk in

Peer-reviewed version available at *Proteomes* **2018**, *6*, 52; doi:10.3390/proteomes6040052

the biofilm milieu. We used a proteomic approach to gain the first insights into how this clinically rarely identified bacterium interacts with other bacteria and its human host.

Methods

Ethics Statement. A human subject protocol, together with a consent form explaining risks of participation in the study, was generated by the Southwest Regional Wound Care Center (SRWCC) in Lubbock, TX and the J. Craig Venter Institute (JCVI) in Rockville, MD. The study number was #56-RW-022. The Western Institutional Review Board (WIRB) in Olympia, Washington and the IRBs of the JCVI and Northeastern University (NEU) in Boston, MA approved the protocol in 2013. All enrolled adults provided written consent. Catheter specimens were collected firsthand for the study. A medical need to replace the Foley catheters in patients in the context of bladder management existed. Scientists who analyzed specimens via microbial culture and proteomic analyses (at the research sites JCVI and NEU) did not have access to data allowing patient identification. Electronic and printed medical records created at SRWCC were retained for four years to facilitate integrated reviews of medical data and scientific research results and then destroyed.

Clinical background and patient specimens. The parent study was prospective and included nine patients who contributed indwelling catheter samples collected longitudinally over a time frame of 3 to 6 months. The patients suffered from neurogenic bladder syndrome as well as chronic wounds. Treatment of these pathologies were the reasons for regularly scheduled visits of the wound clinic. Routine care included catheter exchange to minimize the risk of CAUTI. By performing 16S rRNA and proteomic analyses on series of catheter extracts, the genus *Actinotignum* was identified from CB samples derived from two male subjects (P1 and P5).

Peer-reviewed version available at Proteomes 2018, 6, 52; doi:10.3390/proteomes6040052

Catheter sample processing for microbial cultures, 16S and proteomics. Catheters specimens were cut into one-inch pieces. Two methods were used to process catheter samples, one with the objective to proceed with culture-free metagenomic and proteomic analyses and the other with the objective to isolate and grow fastidious anaerobic and microaerophilic microbes. Immediately after collecting the catheter specimens, samples for culture-free 'omics analyses were placed in polypropylene tubes, stored at -20˚C for 6-24 h prior to shipment to JCVI on ice and frozen at -80˚C until the day of sample extractions. For cultures of fastidious microbial organisms, samples were preserved differently. Freshly collected catheter specimens were placed into Balch glass test tubes filled with 10 mL sterile anaerobic basic medium with urea (BMU). The tubes were flushed with Nitrogen gas, sealed with a rubber stopper, capped and delivered to the lab at NEU via overnight shipment at ambient temperatures. BMU media (pH 6) contained the following components in g/L: yeast extract, 0.1; Casamino Acids, 0.1; KH_2PO_4, 2.1; K_2HPO_4, 6.35; urea, 0.1; $MgCl_2 \times 6\ H_2O$, 0.1; NH_4Cl, 0.4; $CaCl_2 \times 2\ H_2O$, 0.05; trace elements SL10, 1 ml/L; $FeCl_2 \times 4\ H_2O$, 0.05; L-cysteine-HCl, 0.5; resazurin 0.0025. Upon arrival of the tube in the lab, it was placed in an anaerobic glove cabinet, vortexed to homogenize the microbial suspension and serially diluted. BMU dilutions were plated onto anaerobic trypticase-yeast extract agar plates supplemented with L-cysteine-HCl as a reducing agent and sheep blood (25 mL/L). The trypticase-yeast extract (TY) agar composition in g/L was as follows: trypticase, 20.0; yeast extract, 10.0; agar, 15; $FeCl_2 \times 4\ H_2O$, 0.05; L- cysteine-HCl, 0.5. To propagate growth of fastidious anaerobic bacteria, fresh samples were also inoculated into BMU liquid media supplemented with 1% of human serum, incubated at 37˚C for 7-10 days and then plated on anaerobic TY-blood agar.

***In vitro* liquid culture of *Actinotignum massiliense* in rich growth media.** After up to 10 days of incubation, single colonies were picked from plates with a sterile loop and re-inoculated into liquid TY media supplemented with 1% of human serum for sub-culturing. All steps were conducted in an

anaerobic glove box. From sub-cultures of one facultative anaerobic bacterial colony, *A. massiliense* was identified by 16S rRNA sequencing. From a culture stock (a TY agar colony stored in trypticase-yeast extract at -80˚C), the bacterium was grown anaerobically in 10 mL liquid trypticase soy broth (#43592; Sigma-Aldrich) without agitation overnight at 37˚C. The cultured cell density (OD_{600}) was not determined. The cells were collected via centrifugation at 3,200 × g for 15 minutes at ambient temperature and washed with PBS prior to storage of the cell culture pellet (CCP) at -80˚C and shipment to JCVI.

Catheter biofilm extraction. Urethral latex catheter pieces were thawed. Additional urine pellet (UP) samples derived from catheter bags the patients used were also available and processed as reported previously [11]. Each catheter piece was thawed and placed in a 15 mL Falcon tube with 2-3 mL CHO buffer (100 mM sodium acetate, 20 mM sodium meta-periodate and 300 mM NaCl; pH 5.5). At ambient temperature, the CHO-suspended catheter piece was sonicated in a water bath for 10 minutes allowing the CB biomass to detach from the latex surface and subsequently vortexed. Residual biomass was scraped off the surface with a plastic spatula. The sonication and vortex steps were repeated. The pH of this extract was adjusted to ~ 6.5 to 7.5 with 1 M Tris-HCl (pH 8.1). Centrifugation at 8,000 × g for 15 minutes allowed the recovery of a supernatant (CB_{sup}) and a pellet (CB_{pel}) fraction. The volume of the CB_{sup} fraction was reduced to ~ 0.5 ml in an Ultrafree-4 filter unit (10 kDa MWCO) via centrifugation at 3,200 × g followed by buffer exchange into PBS. The CB_{pel} fraction was not re-suspended. Both fractions were stored at -80˚C until further use.

Cell lysis and preparation of CCP and CB lysates for proteomics. CB_{pel}, UP and CCP samples were lysed with the SED solution (1% aqueous SDS, 5 mM EDTA and 50 mM DTT) in low-bind microcentrifuge tubes in a 1:5 volume ratio. Each sample was sonicated in a Misonex 3000 water bath sonicator (ten 30s on/off cycles at amplitude 6.5), then moved to a heat block (95˚C) for 3

Preprints (www.preprints.org) | NOT PEER-REVIEWED | Posted: 26 September 2018 doi:10.20944/preprints201809.0500.v1

Peer-reviewed version available at Proteomes 2018, 6, 52; doi:10.3390/proteomes6040052

minutes and finally incubated to complete lysis with intermittent vortex steps at 20˚C for 15 minutes. Lysates were cleared by centrifugation at 13,100 × g for 10 minutes. Aliquots were subjected to SDS-PAGE to visualize protein bands and estimate the total protein concentration by staining with Coomassie Brilliant Blue-G250 (CBB). A 2 µg BSA lane served as a standard to estimate protein quantity from CBB lane intensity. CB_{sup} fractions were also run in SDS-PAGE gels. Lysate aliquots containing approximately 100 µg total protein were subjected to filter-aided sample preparation (FASP) in single-tube Vivacon filters (10 kDa MWCO membrane; Sartorius AG, Germany), and sequencing-grade trypsin was used to degrade the proteins as reported previously [12]. FASP-processed peptide mixtures were desalted using the Stage-Tip method [13]. The peptide mixtures were lyophilized and then ready for LC-MS/MS analysis.

Shotgun proteomics using LC-MS/MS. Lyophilized peptide mixtures were re-suspended in 10 µl 0.1% formic acid (solvent A). The LC-MS/MS workstation was composed of the LTQ-Velos Pro ion-trap mass spectrometer coupled to the Easy-nLC II system via a FLEX nano-electrospray ion source (Thermo Scientific, San Jose, CA). Detailed LC-MS/MS analysis steps were previously described [14]. The sample was loaded onto a C_{18} trap column (100 µm × 2 cm, 5 µm pore size, 120 Å) and separated on a PicoFrit C_{18} analytical column (75 µm × 15 cm, 3 µm pore size, 150 Å) at a flow rate of 200 nL/min. Starting with solvent A, a linear gradient from 10% to 30% solvent B (0.1% formic acid in acetonitrile) over 195 minutes was followed by a linear gradient from 30% to 80% solvent B over 20 minutes and re-equilibration with solvent A for 5 minutes. The column was washed thrice with a 30-minute solvent A to B linear gradient to minimize carry-over of peptides from sample to sample. Peptide ions were analyzed in a MS^1 data-dependent mode to select ions for MS^2 scans using the software application XCalibur *v2.2* (Thermo Scientific). The ion fragmentation mode was collision-activated dissociation with a normalized collision energy of 35%. Dynamic exclusion was enabled. MS^2 ion scans for the same MS^1 *m/z* value were repeated once and then excluded from

Preprints (www.preprints.org) | NOT PEER-REVIEWED | Posted: 26 September 2018 doi:10.20944/preprints201809.0500.v1

Peer-reviewed version available at Proteomes 2018, 6, 52; doi:10.3390/proteomes6040052

further analysis for 30s. Survey (MS^1) scans ranged from the *m/z* range of 380 to 1,800 followed by MS^2 scans for the selected precursor ions. The ten most intense peptide ions were fragmented in each cycle. Ions that were unassigned or had a charge of +1 were rejected from further analyses. At least two technical LC-MS/MS replicates were run for a sample. Raw MS files from the replicate analyses were combined for the database search step.

Computational methods to profile and quantify metaproteomes. Raw MS files were searched using the Sequest HT algorithm integrated in the software tool Proteome Discoverer v1.4 (Thermo Scientific). Technical parameters and database construction have been described previously [12,15]. Only rank-1 peptides with a length of at least seven amino acids were considered for analysis. The FDR rates were estimated using the Percolator tool in Proteome Discoverer v1.4 with a (reverse sequence) decoy database. Protein hits identified with a 1% FDR threshold were accepted, and the 'protein grouping' function was enabled to ensure that only one protein was reported when multiple proteins shared the same set of identified peptides. The initial database searches without prior knowledge of the present microbial organisms were performed using reviewed protein entries of the non-redundant Homo sapiens UniProt dataset (release 2015-06; 20,195 sequences) and protein sequence entries for 23 microbial genomes, available from the UniProt Proteome data repository, for species that are the common urogenital tract-colonizing microbial species including *A. schaalii* strain CCUG 27420 (UniProt ID UP000035032) (Supplemental File S1). Based on the initial results, datasets with more than ten identified *A. schaalii* proteins were re-analyzed with modifications to the database to verify the *Actinotignum/Actinobaculum spp.* in the sample. Two additional species were reported to colonize the human host: *A. urinale* (strain UMB0759; UniProt ID UP000235308) *and A. massiliense* (strain ACS-171-V-COL2; UniProt ID UP000009888). A third stage of computational analysis pertained to using only those species which, based on 16S rRNA and preliminary proteomic results, were

confidently identified in a sample. This multi-step approach served to minimize incorrect assignments of identical peptides to proteins of origin by the Proteome Discoverer software. This is most important when orthologous proteins with high sequence identities are present in a database, typically an issue with phylogenetically highly related organisms. For the quantitative proteomic analysis, CB_{sup} and CB_{pel} Proteome Discoverer v1.4 output files were merged. We selected the peptide-spectral match (PSM) counts pertaining to the *A. massiliense* proteome to compare clinical (CB) and cell culture (CCP) datasets. Human proteins in CB datasets were also quantified. The normalization across all samples was done based on the division of the PSMs for protein i by the sum of all PSMs in that dataset (PSMi/∑PSM).

16S rRNA analysis. All CB_{pel} samples (5-25 µL volume) were re-suspended in 300 µL TES buffer (20 mM Tris-HCl, pH 8.0, 2 mM EDTA, and 1.2% Triton X-100), vortexed occasionally and incubated at 75°C for 10 minutes. To the cooled CB_{pel} suspension, 60 µL chicken egg lysozyme (200 µg/mL), 5.5 µL mutanolysin (20 U/mL; Sigma Aldrich) and 5 µL linker RNase A were added. An incubation for 60 min at 37˚C was followed by addition of 100 µL 10% SDS and 42 µL proteinase K (20 mg/mL). Bacteria in these suspensions were lysed overnight at 55˚C. A standard DNA extraction procedure with phenol-chloroform-isoamylalcohol (25:24:1), centrifugation at 13,100 x g for 20 minutes and recovery of the aqueous phase to enrich bacterial DNA followed. Nucleic acids were salted out by adding 3 M sodium acetate (pH 5.2). DNA was precipitated by adding an equal volume of ice-cold isopropanol, pelleted by spinning at 13,000 x g for 10 minutes, washed with 80% ethanol, and resuspended in TE buffer for storage at -20˚C. DNA library preparation for the amplification of V1-V3 regions of 16S rRNA bacterial genes and the MiSeq (Illumina) sequencing approach were described previously [16]. With UPARSE for phylogenetic analysis [17], operational taxonomic units (OTUs) were generated *de novo* from raw sequence reads using default parameters in UPARSE, the Wang classifier and bootstrapping using 100 iterations. Taxonomies were assigned to the OTUs

with Mothur applying the SILVA 16S rRNA database version 123 as the reference database [18]. Unbiased, metadata-independent filtering was used at each level of the taxonomy by eliminating samples with less than 2000 reads.

Protein function and biological pathway analyses. The annotation of protein-encoding genes in the reference proteome *A. massiliense* ACS-171-V-COL2 [10] is preliminary, and many proteins are annotated as uncharacterized. We conducted sequence homology searches with BlastP in UniProt to identify bacterial orthologs with gene identifiers and putative functional roles. The Metacyc.org and Ecocyc.org databases were used to infer relationships of proteins with distinct biological pathways. Assessing both frequency of identification of proteins part of a pathway and relative abundance of the *A. massiliense* proteins, we inferred the activity of biosynthetic and metabolic pathways in the CB milieu. Assessing the predicted presence of signal sequences, cell wall localization motifs and transmembrane domains as well as the location of genes in clusters, we obtained additional data indicate of a protein's functional role.

Results

Actinobaculum massiliense is a recurrent colonizer of catheter surfaces part of a polymicrobial biofilm. For patients P1 and P5 who were part of a study to understand the microbial complexity of urethral CBs in a hostile host milieu, we observed *A. massiliense* as a cohabitant of polymicrobial biofilms. In three sequentially replaced catheters from P1, *A. massiliense* was a component of the CB community joined by *Proteus mirabilis*, *Escherichia coli* and *Enterococcus faecalis*. In five sequentially replaced catheters from P5, the bacterium colonized CB surfaces together with all or some of the following species: *P. mirabilis*, *E. coli*, *E. faecalis*, *Aerococcus urinae*, *Streptococcus agalactiae* and *Propionimicrobium lymphophilum* (Fig. 1). The 16S rDNA surveys are sensitive with respect to the amplification of the *Actinotignum/Actinobaculum* 16S rRNA V1-V3 region. This data

Preprints (www.preprints.org) | NOT PEER-REVIEWED | Posted: 26 September 2018 doi:10.20944/preprints201809.0500.v1

Peer-reviewed version available at Proteomes 2018, 6, 52; doi:10.3390/proteomes6040052

revealed that the genus was present in six and eight sequentially collected CB/UP samples from P1 and P5, respectively, thus confirming the proteome analyses. We learned that *A. massiliense* is a recurrent colonizer of indwelling urethral catheters, invariably as a component of a polymicrobial community. The bacterial biofilm appears to persist via adhesion to the urothelial mucosa during catheter replacement in a patient and is altered in its quantitative composition over time (Fig. 1). Actinobacteria (*A. massiliense* and *P. lymphophilum*) are low to medium abundance contributors to the biofilms and appear to be unable to become dominant strains in the CB microbial biomass.

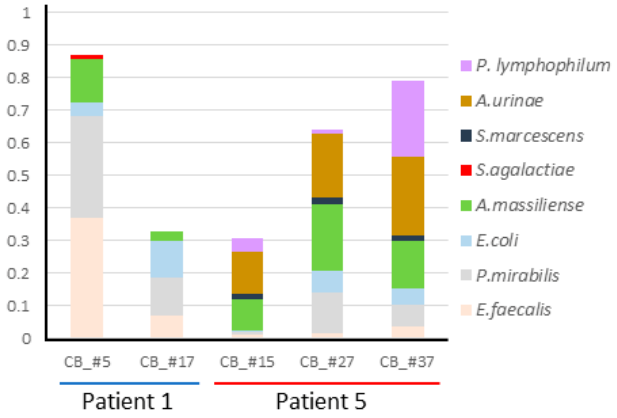

Fig. 1. Quantitative representation of microbial proteomes in CB samples. The bars are ordered from left to right according to the sequential collection time points. For patient 1, the time points were a week apart; for patient 5, the time points were a month apart. Number gaps do not indicate missed samples. Colored segments of bars represent the relative contribution of a microbial species to the entire proteome (including human). The legend on the right links the color in the graphic to the identified species.

Actinobaculum massiliense is a fastidious bacterium favoring anaerobic growth. A few of the clinical specimens were subjected to microbial culture on blood agar preserving and growing the viable microbes under anaerobic conditions or aerobic conditions. While we did not isolate *A. massiliense* colonies from catheter specimens frozen and re-thawed incubating under ambient conditions or with 5% CO_2, we isolated *A. massiliense* colonies after preserving the catheters in nitrogen-flushed and sealed tubes to maintain anaerobicity followed by growth within 24 h on blood agar in an anaerobic chamber. Small grey colonies visible on blood agar were isolated after 48 hr of growth were

Preprints (www.preprints.org) | NOT PEER-REVIEWED | Posted: 26 September 2018 doi:10.20944/preprints201809.0500.v1

Peer-reviewed version available at Proteomes 2018, 6, 52; doi:10.3390/proteomes6040052

analyzed by 16S rRNA sequencing and identified as *A. massiliense*. As the image of Fig. 2 shows, many bacterial species with distinct colony morphologies grew in the anaerobic milieu, consistent with low levels of oxygen urethral catheter biofilm-colonizing microbes are exposed to.

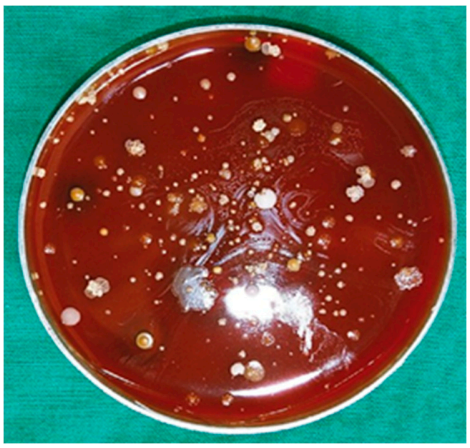

Fig. 2. Anaerobically grown microorganisms derived from a urethral catheter sample of patient 5 on a blood agar plate. Within 48 hr various colonies emerged. Among those identified by 16S rRNA analysis on the genus or species level were: *Actinobaculum massiliense, Actinomyces sp., Aerococcus sp., Enterococcus sp., Escherichia coli, Finegoldia sp., Morganella morganii, Porphyromonas asaccharolytica,* and *Prevotella timonensis*.

Proteomic analysis of *Actinobaculum massiliense* from growth in nutrient-rich media and clinical samples. To our knowledge, we characterize the proteome of any *Actinotignum/Actinobaculum* species, derived from *in vitro* or *in vivo* growth environments, for the first time. We examined four *A. massiliense* proteomic datasets associated with CB extracts, two each pertaining to samples from patients P1 and P5. Their composition is expected to reflect bacterial adaptations to the nutrient conditions in the urinary tract. In addition to inorganic salts, urine is rich in urea, organic and amino acids. The fluid contains peptide breakdown products of proteins, glucuronate-conjugated toxins and pigments (e.g. urobilin), which are mostly derived from renal metabolic and excretion processes [19]. Urothelial mucosal surface glycoproteins and breakdown products and the CB matrix also contribute to the pool of nutrients. We compared the *in vivo* proteomes with an isolate of *A. massiliense* (P5) that was grown planktonically to stationary phase in sugar- and amino acid-rich

Preprints (www.preprints.org) | NOT PEER-REVIEWED | Posted: 26 September 2018 doi:10.20944/preprints201809.0500.v1

Peer-reviewed version available at Proteomes 2018, 6, 52; doi:10.3390/proteomes6040052

media. All proteomic datasets are provided in Supplemental File S2, with protein identities as annotated for the genome of strain ACS-171-V-Col2 and their PSM-based quantities. Overall, 759 proteins with at least two unique peptides, representing 44.7% of the *in silico* predicted proteome, were identified; 739 and 585 proteins were identified from the *in vitro* and the combined *in vivo* datasets, respectively. *In vivo vs. in vitro* abundance differences were observed for many proteins, in support of the notion that *A. massiliense* modulates its proteome to grow as a CB constituent, competing with other bacteria for nutrients in an anoxic, hostile host milieu that features prolonged infiltration of innate immune cells into the urothelial mucosa. Due to limited protein descriptions for 1,696 unreviewed TremBL entries predicted for the genome of strain ACS-171-V-Col2, we assessed the biological roles of proteins further from data on conserved domains (information in UniProt) and sequence homology searches to identify better annotated orthologs. Furthermore, we inferred the subcellular localizations of some proteins from transmembrane, secretion signal and cell wall anchor motifs. Prioritizing proteins that potentially interact with the human host or are important for bacterial fitness in the urinary system, a list of proteins, many of which were found to be abundant *in vivo*, are selected here (Table 1).

Table 1. *Actinobaculum massiliense* proteins potentially participating in the crosstalk with the host.

Gene locus [1]	Protein description [2]	Functional group or domain [3]	Put. role in inter-action with host [4]	Predict. location [5]	Q (ivv vs ivt) [6]	Q avg (ivv) [7]
01095	Putative subtilisin-like protease	fibronectin type III, S8pro	invasion, inflammation	CW; SP motif	>8	0.0617
00826	Rib/alpha/Esp surface antigen repeat-containing protein	Ca^{2+}/cadherin bndg type III repeat and Ig-like fold	adhesion, biofilm formation	CW; SP motif	>8	0.0434
00810	Putative subtilisin-like protease	fibronectin type III, S8pro	invasion and inflammation	CW; SP motif	2-8	0.0406
01185	Oligopeptide/nickel binding protein	ABC transporter su., MppA-type	metal/heme/ peptide uptake	CW; SP motif	2-8	0.0230
01650	L-arginine:glycine amidinotransferase	creatine synthesis from arginine	part of PKS pathway	CY	>8	0.0196
00827	Rib/alpha/Esp surface antigen repeat-containing protein	Ca^{2+}/cadherin bndg type III repeat	adhesion, biofilm formation	CW; SP motif	2-8	0.0092

Preprints (www.preprints.org) | NOT PEER-REVIEWED | Posted: 26 September 2018 doi:10.20944/preprints201809.0500.v1

Peer-reviewed version available at Proteomes 2018, 6, 52; doi:10.3390/proteomes6040052

01410	Bacterial Ig-like domain protein	Ig-like domain	adhesion	not predicted	2-8	0.0047
01413	Listeria-Bacteroides repeat domain	Cadherin E-binding domain	adhesion, invasion	CW; SP motif	2-8	0.0045
01648	Ornithine carbamoyltransferase (ArcB)	arginine metabolism	part of PKS pathway	CY	>8	0.0042
00680	Oligopeptide/nickel binding protein	ABC transporter su., MppA-type	metal/heme/ peptide uptake	CW; SP motif	<2	0.0038
01649	Carbamate kinase (ArcC)	arginine metabolism	part of PKS pathway	CY	>8	0.0034
01184	Oligopeptide ABC transporter, ATP-binding domain	ABC transporter su.	metal/heme/ peptide uptake	CM	<2	0.0031
00954	Papain-like cysteine protease	cysteine protease	extracellular proteolysis	not predicted	2-8	0.0023
00866	LPXTG-domain-containing cell wall anchor protein	pilin subunity D1 domain	adhesion	LPLTG CW anchor	2-8	0.0022
01647	Arginine deiminase (ArcA)	arginine metabolism	part of PKS pathway	CY	>8	0.0021
01182	Oligopeptide ABC transporter, permease	ABC transporter su.	metal/heme/ peptide uptake	CM	2-8	0.0017
00677	Oligopeptide ABC transporter, ATP-binding domain	ABC transporter su.	metal/heme/ peptide uptake	CM	<2	0.0017
01364	Putative polyketide synthase	multifunctional enzyme	polyketide biosynthesis	CY	<2	0.0015
00649	Fe/B12 periplasmic binding protein	ABC transporter su., FecB-like	metal/cofactor uptake	CW; SP motif	>8	0.0015
00581	LPXTG-domain-containing cell wall anchor protein	G5 repeat domains	cell surface modulation	LPHTG CW anchor	>8	0.0014
01361	Biotin-[acetyl-CoA-carboxylase] ligase	part of PKS pathway	part of PKS pathway	CY	<2	0.0012
00678	Oligopeptide ABC transporter, ATP-binding domain	ABC transporter su.	metal/heme/ peptide uptake	CM	<2	0.0010
01183	Oligopeptide ABC transporter, permease	ABC transporter su.	metal/heme/ peptide uptake	CM	<2	0.0005
01418	Oligopeptide/nickel binding protein	ABC transporter su., MppA-type	metal/heme/ peptide uptake	CW; SP motif	>8	0.0004
00679	Oligopeptide ABC transporter, permease	ABC transporter su.	metal/heme/ peptide uptake	CM	<2	0.0004
01362	ATP grasp family protein	part of PKS pathway	part of PKS pathway	CY	<2	0.0003

Proteins are listed according to abundance *in vivo*. [1] gene locus (prefix HMPREF9233_); [2] description from its annotation or that of an orthologous protein; [3] functional role based on the entire sequence or a domain (data were from UniProt, GO term and/or InterPro references), su.=subunit; [4] putative interactions with the host based on data from [2, 3, 5], PKS=polyketide synthesis; [5] predicted subcellular localization based on signal sequence for export or cell wall

Preprints (www.preprints.org) | NOT PEER-REVIEWED | Posted: 26 September 2018 doi:10.20944/preprints201809.0500.v1

Peer-reviewed version available at *Proteomes* **2018**, *6*, 52; doi:10.3390/proteomes6040052

anchorage, CY=cytosol, CW=cell wall, CM=cell membrane, SP=signal peptide; [6] range of abundance ratios *in vivo* (ivv) *vs. in vitro* (ivt); [7] estimated relative protein quantity derived from four *in vivo* (ivv) datasets using the ratio PSMi/∑PSM.

Potentially direct *A. massiliense* protein interactions with host environment. Two putative subtilisin-like proteases (gene loci 01095 and 00810) were highly abundant in the CB (*in vivo*) samples. The protease 01095 was on average 230-fold more abundant *in vivo* than in cell culture (*in vitro*), the protease 00810 was 2.4-fold more abundant. Fig. 3 shows the sequence coverage for the protease 01095 from one dataset. Lack of sequence coverage in the 200 N-terminal amino acids suggests a preproenzyme, with a predicted signal peptide cleavage site at $A_{29}D$ and a propeptide between D_{30} and ~ K_{197} that enables enzyme activation. The two proteases have high (32%) sequence identity (BlastP E-values 1e-97 and 8e-104, respectively) with lactocepin, a *Lactobacillus paracasei* protease exerting anti-inflammatory effects by degrading proinflammatory cytokines in the human gastrointestinal tract [20]. Of note, proteomic data showed evidence of complement system activity and the infiltration of neutrophils and in the urinary tract of P1 and P5. Both effector proteins and cytokines released by innate immune cells may be susceptible to cleavage by these subtilisin-like proteases [21]. Table 2 lists the twenty-five on average most abundant proteins in the four *in vivo* datasets.

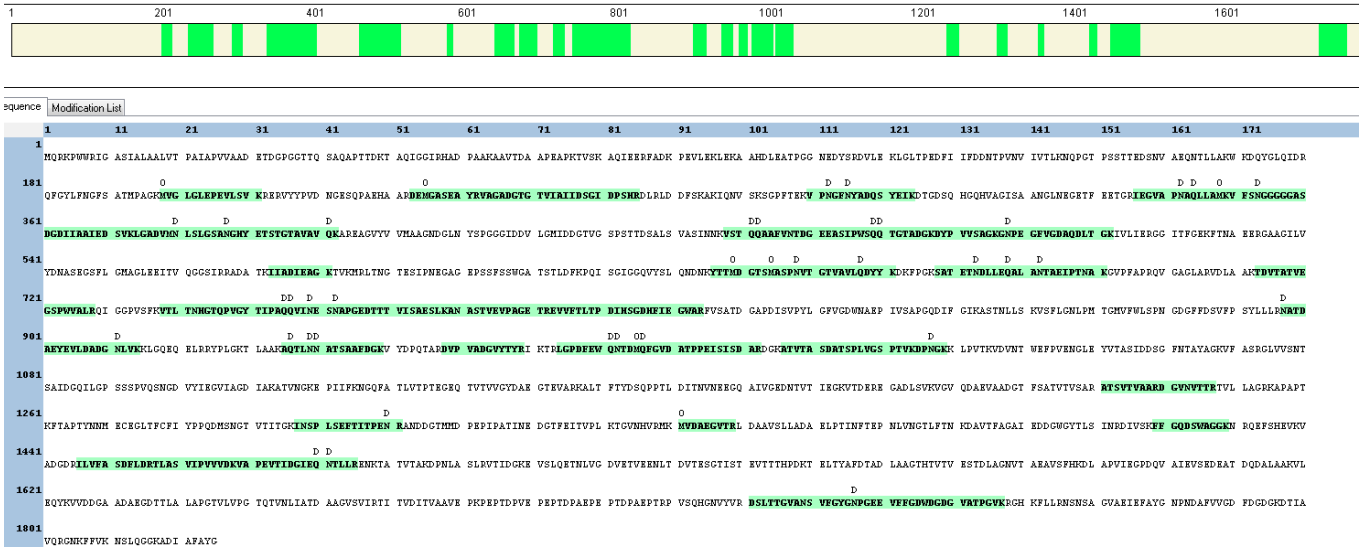

Preprints (www.preprints.org) | NOT PEER-REVIEWED | Posted: 26 September 2018 doi:10.20944/preprints201809.0500.v1

Peer-reviewed version available at Proteomes 2018, 6, 52; doi:10.3390/proteomes6040052

Fig. 3. HMPREF9233_01095 protein sequence (putative subtilisin-like protease). The peptides identified in the shotgun proteomic analysis are highlighted in green in bar and peptide sequence formats. Amino acid modifications are listed above the identified sequences, including deamidation (D) and methionine oxidation (O). The modifications may have occurred during sample analysis and not reflect biological changes.

Table 2. Abundant human proteins in catheter biofilm extracts with *A. massiliense* contributions.

Accession [1]	Description [2]	Average CB [3]
P02768	[6] Serum albumin = ALB [ALBU_HUMAN]	0.0793
P02788	[4,7] Lactotransferrin = LTF [TRFL_HUMAN]	0.0365
P13645	[5] Keratin, type I cytoskeletal 10 = KRT10 [K1C10_HUMAN]	0.0333
P05164	[4] Myeloperoxidase = MPO [PERM_HUMAN]	0.0314
P06702	[4] Protein S100-A9 = S100A9 [S10A9_HUMAN]	0.0306
P04264	[5] Keratin, type II cytoskeletal 1 = KRT [K2C1_HUMAN]	0.0293
P01834	[6,8] Immunoglobulin kappa constant chain = IGKC [IGKC_HUMAN]	0.0200
P0DOX5	[6,8] Immunoglobulin gamma-1 heavy chain [IGG1_HUMAN]	0.0191
P02538	[5] Keratin, type II cytoskeletal 6A = KRT6A [K2C6A_HUMAN]	0.0187
P04259	[5] Keratin, type II cytoskeletal 6B = KRT6B [K2C6B_HUMAN]	0.0173
P35908	[5] Keratin, type II cytoskeletal 2 epidermal = KRT2 [K22E_HUMAN]	0.0167
P59665	[4,7] Neutrophil defensin = DEFA1 [DEF1_HUMAN]	0.0165
P02787	[6] Serotransferrin = TF [TRFE_HUMAN]	0.0151
P0DOX7	[6,8] Immunoglobulin kappa light chain [IGK_HUMAN]	0.0151
P01024	[8] Complement C3 =C3 [CO3_HUMAN]	0.0146
P13646	[5] Keratin, type I cytoskeletal 13 = KRT13 [K1C13_HUMAN]	0.0143
P13647	[5] Keratin, type II cytoskeletal 5 OS = KRT5 [K2C5_HUMAN]	0.0137
P02533	[5] Keratin, type I cytoskeletal 14 = KRT14 [K1C14_HUMAN]	0.0121
P08779	[5] Keratin, type I cytoskeletal 16 = KRT16 [K1C16_HUMAN]	0.0116
P01876	[6,8] Immunoglobulin heavy constant alpha 1 = IGHA1 [IGHA1_HUMAN]	0.0114
P02675	[8] Fibrinogen beta chain = FGB [FIBB_HUMAN]	0.0112
P02679	[8] Fibrinogen gamma chain = FGG [FIBG_HUMAN]	0.0109
P01861	[6,8] Immunoglobulin heavy constant gamma 4 = IGHG4 [IGHG4_HUMAN]	0.0107
P05109	[4] Protein S100-A8 = S100A8 [S10A8_HUMAN]	0.0101
P08311	[4] Cathepsin G = CTSG [CATG_HUMAN]	0.0101

Proteins are ordered based on average abundance *in four in vivo proteomic datasets with evidence of A. massiliense colonization*. [1]UniProt ID; [2]descriptions from annotation; [3]normalized quantities derived from the four *in vivo* (ivv) datasets using PSMi/∑PSM; [4]proteins abundant in activated neutrophils; [5]proteins abundant in keratinizing epithelial cells and variably expressed by urothelial cells; [6]proteins abundant in normal urine; [7]proteins also secreted by urothelial umbrella cells upon pathogen recognition; [8]proteins released during inflammatory response via tissue injury or active secretion. The information on cell-specific expression, extracellular release and excretion via glomerular filtration is derived from Protein Atlas (www.proteinatlas.org) and selected literature [22-24]

Peer-reviewed version available at *Proteomes* **2018**, *6*, 52; doi:10.3390/proteomes6040052

Two Rib/alpha/Esp surface antigen repeat-containing proteins encoded by adjacent gene loci (00826 and 00827) were also abundant in the CB proteomes. The protein 00826 was on average 13-fold more abundant *in vivo* than *in vitro*, the protein 00827 was 3.8-fold more abundant. Both have Ca^{2+}-dependent cadherin-like domains which are known to promote cell adhesion processes and are truncated compared to a better characterized ortholog, the *E. faecalis* Esp surface protein (EF0056). The sequences of Esp and 00826 are 39% identical in the aligned protein regions (e-value 0.018). *E. faecalis* Esp promotes formation of biofilms on catheter bag surfaces [25]. The protein 00826 has calcium-binding type 3 (T3) repeats. The ORF 00828 (82 amino acids) has a LPHTG motif suggesting sequence/assembly errors and a gene with ORFs 00827 and 00828 encoding a single cell wall-anchored protein with an adhesion function. Two additional LPXTG motif proteins (gene loci 00581 and 00866) whose N-terminal domains have no functional role predictions were identified. In LPXTG peptide sequences, carboxyl termini of the threonine residue are coupled to amino groups of a peptide side chain part of the cell wall peptidoglycan. N-terminal segments of such proteins are typically exposed at the bacterial cell surface and interact with the extracellular environment. The protein 00581 was more abundant in the *in vivo* proteomes compared to that of *A. massiliense* grown *in vitro*. A high M_r, putative polyketide synthase (PKS), located in gene locus 01364, was expressed *in vivo* and *in vitro*. Interestingly, along with several enzymes participating in arginine metabolism, a L-arginine:glycine amidinotransferase was highly abundant *in vivo*. An ortholog of the enzyme was reported to contribute to the biosynthesis of a *Cylindrospermopsis raciborskii* polyketide hepatotoxin [26]. Enzymes expressed from two gene clusters and potentially implicated in polyketide synthesis by *A. massiliense* are shown in the schematic of Figure 4. PKSs require a pantothenate cofactor for thiol transfer reactions, and enzymes for a pathway to generate this cofactor were expressed. Whether a functional link between PKS and amidinotransferase leading to the production of a currently uncharacterized polyketide-type secondary metabolite exists

Preprints (www.preprints.org) | NOT PEER-REVIEWED | Posted: 26 September 2018 doi:10.20944/preprints201809.0500.v1

Peer-reviewed version available at Proteomes 2018, 6, 52; doi:10.3390/proteomes6040052

362 remains to be determined. Such a metabolite may act as a siderophore or cytotoxin, representing
363 functions in iron acquisition and inter-microbial competition, respectively.
364
365 *A. massiliense* pathways with roles in nutrient acquisition in CB milieu derived from proteomic data.
366 Surveying the *in vivo* expressed proteomes of *A. massiliense* for putative transport functions, we
367 identified oligopeptide transporters encoded by the gene loci 00677-00680 and 01182-01185
368 (Figure 4). Of the two abundant Mpp-type substrate binding proteins, 00680 and 01185, 01185 was
369 moderately increased in CBs compared to *in vitro* growth conditions. Mpp domain assignments
370 suggest import of oligopeptides or heme. Heme and metal ions are sequestered by the human host
371 to prevent bacterial growth. In Table 2, two such proteins LTF (sequestering Fe^{3+}) and S100-A8
372 (sequestering Ca^{2+}) are listed. A predicted periplasmic Fe/B12-binding protein (00649) was also
373 identified (Table 1). It was detected in the proteome of biofilms from patient P5 but absent in biofilms
374 from P1 and *in vitro*. If the Mpp-type transporters indeed bind oligopeptides, *A. massiliense* would
375 have not only the protein repertoire to import them but also to digest the peptides: the peptidases
376 M13, M20, PepC1 and PepN and several enzymes degrading amino acids (GdhA, DsdA and IlvE)
377 were of moderate to high abundance in the *in vivo* datasets (Figure 4). PepC1, PepN and M20 have
378 zinc as a cofactor, indicating the need for metal ion uptake to support metabolic processes.

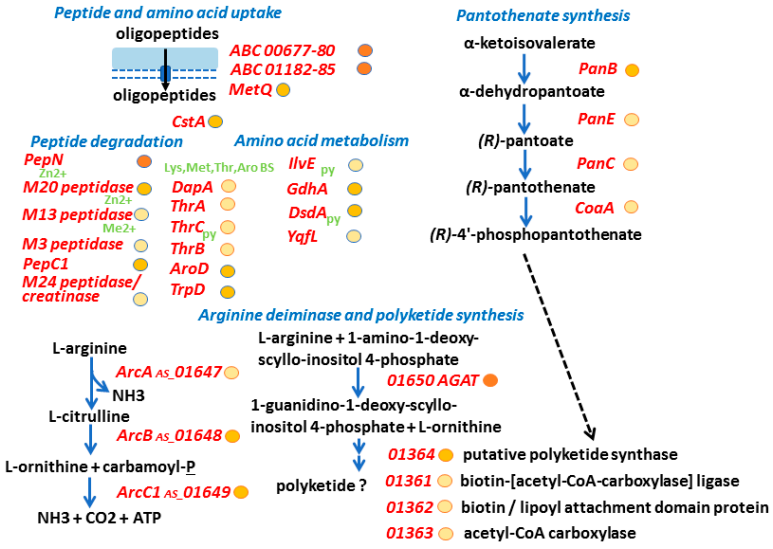

379

Fig. 4. Putative *A. massiliense* peptide uptake, peptide/amino acid metabolism and PKS synthesis functionalities. The schematic contains protein names in red (short names in strain ACS-171-V-Col2 database or those of orthologs) and/or gene loci (no functional predictions were made; last 5 numbers of the accession number). ABC: ABC transporter. The metabolite names are given in black, blue arrows show an enzymatic activity, black arrows a transport activity, and hatched black arrows a cofactor contribution. The darker the color of the circle behind the protein name, the higher the average abundance level of a protein in *in vivo* datasets. Proteins suing cofactor (in green script) are also depicted: Me2+ (metal ion), Zn2+ (zinc), py (pyridoxal-5'-phosphate).

Glycolytic and mixed acid fermentation pathway of *A. massiliense*. Among putative sugar uptake systems, the xylose uptake protein XylF part of an ABC transporter was highly expressed in the CB proteomes. Further support for the relevance of this transporter's sugar substrate assignment was derived from the fact that two enzymes active in this sugar's degradation pathway (XylA and XylB), present in the same gene cluster (00910-00917), were also expressed *in vivo*, and that the aldolase Xfp, cleaving xylulose-phosphate, was also abundant in CB proteomes. This pathway is shown in Fig. 5. Subsequent glycolytic steps and mixed acid fermentation (MAF) were represented in the bacterial proteome, and high expression of the respective enzymes demonstrate the key role of this metabolic pathway for *A. massiliense* in the low-oxygen urinary tract milieu. There was no evidence of an active citrate cycle. More evidence for fermentation activities was associated with the highly expressed enzyme FucO, producing propan-1,2-diole (Fig. 5). *A. massiliense* also had evidence of active glucuronate/gluconate uptake and metabolism *in vivo*, including putative sugar acid uptake systems and D-glucuronate and D-glucarate catabolic pathways. 2-Dehydro 3-deoxy D-gluconate is fed into the glycolytic pathway via activities of KdgK and Eda, both of which were expressed in the CB milieu (Fig. 6). Conjugates of glucuronate are produced in the kidneys to detoxify and excrete hydrophobic waste products into urine. Pyruvate dehydrogenase composed of AceE, AceF and Lpd also appeared to be highly active. Furthermore, the proteomic data yielded support for glycogen synthesis and mobilization activities by *A. massiliense* and the synthesis of dTDP-L-rhamnose, a

Preprints (www.preprints.org) | NOT PEER-REVIEWED | Posted: 26 September 2018 doi:10.20944/preprints201809.0500.v1

Peer-reviewed version available at Proteomes 2018, 6, 52; doi:10.3390/proteomes6040052

406 sugar present in many bacterial surface oligosaccharides *in vivo* (Suppl. File S3). The structure of
407 the rhamnose-containing surface antigen in *A. massiliense* is unknown. The bacterium highly
408 expressed glycolytic enzymes involved in the catabolism of glucose and fructose (data not shown).

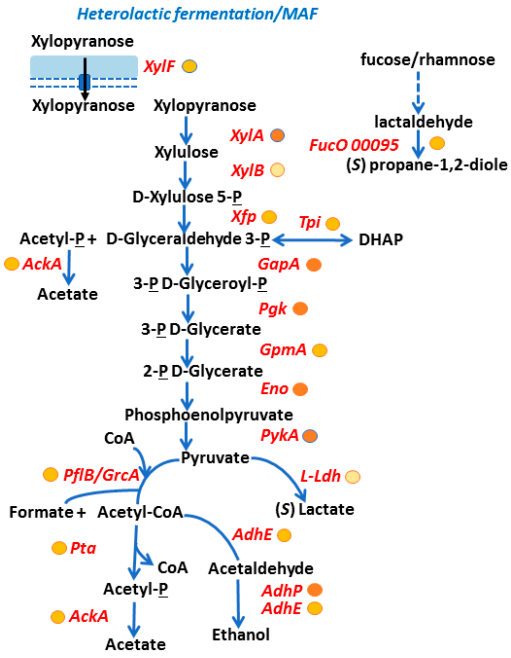

409

410 Fig. 5. Evidence of active *A. massiliense* mixed acid fermentation pathways utilizing xylose *in vivo*. The legends
411 describing the protein and metabolite entities are analogous to those provided for Fig. 4.

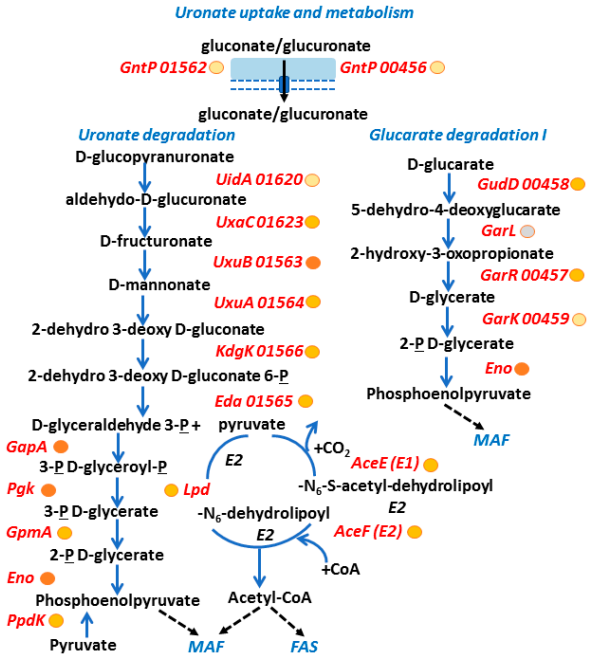

412

Fig. 6. Evidence of active *A. massiliense* glucuronate and glucarate metabolism pathways. The legends describing the protein and metabolite entities are analogous to those provided for Fig. 4. MAF: mixed acid fermentation; FAS: fatty acid synthesis.

Discussion

A. massiliense persists in polymicrobial catheter biofilms in the presence of uropathogens. In five CB extracts derived from long term-catheterized patients whose urethral catheters were sequentially replaced, *A. massiliense* was identified as a cohabitant of polymicrobial CBs with ~ 5-30% microbial biomass contributions according to *in vivo* 16S rRNA and proteomics data. Whether *A. massiliense* is a true pathogen or bystander in cases of infection is a matter of debate [27]. Some case reports support the notion that the phylogenetically related *A. schaalii* is a pathogen of the urinary tract and can cause systemic infections, such as CAUTI, urosepsis, pyelonephritis and osteomyelitis [2,5,28,29]. Considering that *A. schaalii* detection in many clinical cases is associated with additional pathogens, *A. schaalii* has been termed a UTI co-pathogen [30]. We noticed that a comparison of database searches with *A. schaalii* versus *A. massiliense* of the same dataset resulted in 50-fold less protein identifications for *A. schaalii*, suggesting that these bacteria are phylogenetically more different than currently thought. A deeper genomic characterization should follow to determine if *A. massiliense* should be classified as a species of the newly introduced genus *Actinotignum* [6]. *A. massiliense* may share the co-pathogen definition as a cause of UTI and resident in CAUTI biofilms similar to the ascribed role of *A. schaalii* [31]. But it may also have a microbial bystander role in medical device-adapted biofilms. Joint presence of *Actinotignum/Actinobaculum spp.* and *A. urinae* was reported in several infection case reports suggesting their cooperative behavior in the human host environment. Other bacteria such as *E. coli*, *P. mirabilis* and *E. faecalis*, were also co-identified in clinical cases [2,5,29]. The reported data are consistent with our findings on pathogens cohabitating CBs of two long term-catheterized patients.

Innate immune responses, with neutrophils as the major cell type producing cytokines and effector molecules, are responsible for the defense against pathogens invading the human urinary tract [32]. The complement system and fibrinogen are also factors in the pathogenesis of UTI and CAUTI [33,34]. Independent of the diagnosis of UTI systems, pyuria and neutrophil invasion occur in CAUTIs that are asymptomatic [11,35]. The patients we studied were asymptomatic. In the five surveyed proteomes, there was evidence for the infiltration of neutrophils, the release of complement factors and the deposition of fibrinogen on catheter surfaces. Our data did not allow us to assess if the host defensive processes were caused by all present bacteria or only a subset thereof. It is likely that the immune system targets the entire microbial community in catheter biofilms. The *A. massiliense* proteome, and the comparison of *in vivo* and *in vitro* data, suggest that this bacterium not only adapts to the nutritional milieu in CBs but also to the confrontation by hostile host effector proteins. In the CB environment, the two *A. massiliense* strains expressed high quantities of putative host-interacting molecules (the Rib/alpha/Esp surface antigen repeat-containing proteins 00826 and 00827/00828 with cadherin-like adhesion domains), the latter of which contained a LTXTG cell wall localization motif, and two other LPXTG motif proteins with no functional predictions (00866 and 00581). Many characterized LPXTG motif proteins are involved in adhesion, invasion and biofilm formation in, to name a few pathogens, such as *Staphylococcus aureus* [36], *Enterococci* [25,37] and *Listeria monocytogenes* [38]. We hypothesize that *A. massiliense* expresses these proteins at the cell surface to adhere to other bacterial cells, the abiotic latex surface and/or host proteins that are either exposed on the urothelial surface or deposited as part of the biofilm matrix on catheter surfaces. Specific functional roles need to be identified in biochemical and cell biological follow-up experiments.

Of considerable interest is the high *in vivo* expression level of two subtilisin-like proteases which may cleave cytokines that create an inflammatory environment at the urothelial mucosal interface

or complement, neutrophil and eosinophil effector proteins. An ortholog expressed from the gene *prtP* by *Lactobacillus paracasei* was characterized as a bacterial surface protein with proteolytic activities against interferon γ-induced protein 10 kDa (IP-10) and other cytokines [20]. IP-10 is a key cytokine in infectious disease pathogenesis [39]. The protease PrtB was brought into context with a potential anti-inflammatory activity in irritable bowel disease (IBD) by degrading inflammatory cytokines. We hypothesize that the lactocepin-like *A. massiliense* proteases (01095 and 00810) have proteolytic activities that modulate inflammatory conditions and enhance the ability to persist as a biofilm constituent in CBs. The bacterium expresses a predicted PKS that may biosynthesize a molecule with a polyketide or mixed polyketide-oligopeptide structure. An interesting topic is to concept that siderophores, which capture bivalent metal ions in the extracellular milieu, may also be involved in proinflammatory signaling processes and possess direct virulence properties [40]. The *E. coli* proteomes in CBs of P1 and P5 showed evidence of expression of enzyme components for the synthesis of two known siderophores, enterobactin and yersiniabactin.

Finally, the proteomic data allowed us to infer the *A. massiliense* metabolism and energy generation in the CB milieu. Our data strongly supported a preference of anaerobic energy generation pathways because many MAF enzymes were abundant while the TCA cycle enzymes and cytochromes were absent. Among the sugar precursors, there was evidence for the use of pathways for the import and metabolism of xylose, glucoronate and glucarate. In non-diabetic patients, glucose is present in low concentrations in urine. In contrast, xylose and glucoronate are sugars present in glycoproteins and proteoglycans present in urethral, bladder and renal epithelia [41]. Glucuronate conjugate enzymes are abundant in kidneys where they conjugate the organic acid to lipophilic toxins to allow excretion with the urine. Oligopeptides are other kidney excretion products not exhaustively reabsorbed by the tubular system. We profiled Mpp-type oligopeptide transport systems and peptide-degrading proteases at high expression levels in CBs. *A. massiliense* appears to adjust its metabolic systems

to the nutrient repertoire available in urine and the urothelial mucosa. Studies on *E. faecalis* and *E. coli* grown in urine *in vitro* also reported high expression levels of peptide uptake systems [42,43]. The fitness of *E. coli* as a pathogen of the urinary tract was linked to the ability to take up and metabolize glucuronate and sugars present in urothelial glycoconjugates fed into the central carbon metabolism [44]. *A. massiliense* expressed enzymes contributing to glycogen synthesis suggesting transient storage of this carbohydrate until this energy reservoir needs to be mobilized. In summary, our data support the notion that *A. massiliense* is well-adapted to the nutritional milieu in the urinary tract. It is plausible that the bacterium acquires and provides nutrients in exchange with other microbial cohabitants in the biofilms. Further studies are needed to verify how CB cohabitants share metabolites in the process of generating a mutualistic and perhaps cooperative environment.

Acknowledgements

This work was supported by the National Institutes of Health grant R01GM103598 titled “Urethral catheter-associated polybacterial biofilm formation and dispersal”. The funder had no role in study design, data collection and interpretation, or decisions to submit the work for publication. We thank the Ruggles Family Foundation for the support in acquiring the Q-Exactive mass spectrometer. We thank Mr. Manolito Torralba and Mr. Kelvin Moncera for their efforts to sequence 16S rRNAs from clinical samples.

References

1. Greub, G.; Raoult, D. "Actinobaculum massiliae," a new species causing chronic urinary tract infection. *Journal of clinical microbiology* **2002**, *40*, 3938-3941.
2. Gomez, E.; Gustafson, D.R.; Rosenblatt, J.E.; Patel, R. Actinobaculum bacteremia: A report of 12 cases. *Journal of clinical microbiology* **2011**, *49*, 4311-4313.
3. Lawson, P.A.; Falsen, E.; Akervall, E.; Vandamme, P.; Collins, M.D. Characterization of some actinomyces-like isolates from human clinical specimens: Reclassification of actinomyces suis (soltys and spratling) as actinobaculum suis comb. Nov. And description of actinobaculum schaalii sp. Nov. *Int J Syst Bacteriol* **1997**, *47*, 899-903.
4. Cattoir, V. Actinobaculum schaalii: Review of an emerging uropathogen. *J Infect* **2012**, *64*, 260-267.

5. Reinhard, M.; Prag, J.; Kemp, M.; Andresen, K.; Klemmensen, B.; Hojlyng, N.; Sorensen, S.H.; Christensen, J.J. Ten cases of actinobaculum schaalii infection: Clinical relevance, bacterial identification, and antibiotic susceptibility. *Journal of clinical microbiology* **2005**, *43*, 5305-5308.
6. Yassin, A.F.; Sproer, C.; Pukall, R.; Sylvester, M.; Siering, C.; Schumann, P. Dissection of the genus actinobaculum: Reclassification of actinobaculum schaalii lawson et al. 1997 and actinobaculum urinale hall et al. 2003 as actinotignum schaalii gen. Nov., comb. Nov. And actinotignum urinale comb. Nov., description of actinotignum sanguinis sp. Nov. And emended descriptions of the genus actinobaculum and actinobaculum suis; and re-examination of the culture deposited as actinobaculum massiliense ccug 47753t (= dsm 19118t), revealing that it does not represent a strain of this species. *Int J Syst Evol Microbiol* **2015**, *65*, 615-624.
7. Tuuminen, T.; Suomala, P.; Harju, I. Actinobaculum schaalii: Identification with maldi-tof. *New Microbes New Infect* **2014**, *2*, 38-41.
8. Kristiansen, R.; Dueholm, M.S.; Bank, S.; Nielsen, P.H.; Karst, S.M.; Cattoir, V.; Lienhard, R.; Grisold, A.J.; Olsen, A.B.; Reinhard, M.*, et al.* Complete genome sequence of actinobaculum schaalii strain ccug 27420. *Genome Announc* **2014**, *2*.
9. Beye, M.; Bakour, S.; Labas, N.; Raoult, D.; Fournier, P.E. Draft genome sequence of actinobaculum massiliense strain fc3. *Genome Announc* **2016**, *4*.
10. Earl A., W.D., Feldgarden M., Gevers D., Saerens B., Vaneechoutte M., Walker B., Young S.K., Zeng Q., Gargeya S., Fitzgerald M., Haas B., Abouelleil A., Alvarado L., Arachchi H.M., Berlin A., Chapman S.B., Goldberg J. , Griggs A., Gujja S., Hansen M., Howarth C., Imamovic A., Larimer J., McCowen C., Montmayeur A., Murphy C., Neiman D., Pearson M., Priest M., Roberts A., Saif S., Shea T., Sisk P., Sykes S., Wortman J., Nusbaum C., Birren B. The genome sequence of actinobaculum massiliae acs-171-v-col2. 2012-09-12, 2012.
11. Yu, Y.; Zielinski, M.; Rolfe, M.; Kuntz, M.; Nelson, H.; Nelson, K.E.; Pieper, R. Similar neutrophil-driven inflammatory and antibacterial activities for symptomatic and asymptomatic bacteriuria in elderly patients. *Infect Immun* **2015**.
12. Yu, Y.; Suh, M.J.; Sikorski, P.; Kwon, K.; Nelson, K.E.; Pieper, R. Urine sample preparation in 96-well filter plates for quantitative clinical proteomics. *Anal Chem* **2014**, *86*, 5470-5477.
13. Yu, Y.; Smith, M.; Pieper, R. A spinnable and automatable stagetip for high throughput peptide desalting and proteomics. In *Protocol Exchange*, Nature Publishing Group: 2014; Vol. doi:10.1038/protex.2014.1033.
14. Suh, M.J.; Tovchigrechko, A.; Thovarai, V.; Rolfe, M.A.; Torralba, M.G.; Wang, J.; Adkins, J.N.; Webb-Robertson, B.J.; Osborne, W.; Cogen, F.R.*, et al.* Quantitative differences in the urinary proteome of siblings discordant for type 1 diabetes include lysosomal enzymes. *Journal of proteome research* **2015**, *14*, 3123-3135.
15. Yu, Y.; Sikorski, P.; Bowman-Gholston, C.; Cacciabeve, N.; Nelson, K.E.; Pieper, R. Diagnosing inflammation and infection in the urinary system via proteomics. *J Transl Med* **2015**, *13*, 111.
16. Singh, H.; Yu, Y.; Suh, M.J.; Torralba, M.G.; Stenzel, R.D.; Tovchigrechko, A.; Thovarai, V.; Harkins, D.M.; Rajagopala, S.V.; Osborne, W.*, et al.* Type 1 diabetes: Urinary proteomics and protein network analysis support perturbation of lysosomal function. *Theranostics* **2017**, *7*, 2704-2717.
17. Edgar, R.C. Uparse: Highly accurate otu sequences from microbial amplicon reads. *Nat Methods* **2013**, *10*, 996-998.
18. Quast, C.; Pruesse, E.; Yilmaz, P.; Gerken, J.; Schweer, T.; Yarza, P.; Peplies, J.; Glockner, F.O. The silva ribosomal rna gene database project: Improved data processing and web-based tools. *Nucleic Acids Res* **2013**, *41*, D590-596.
19. Bouatra, S.; Aziat, F.; Mandal, R.; Guo, A.C.; Wilson, M.R.; Knox, C.; Bjorndahl, T.C.; Krishnamurthy, R.; Saleem, F.; Liu, P.*, et al.* The human urine metabolome. *PLoS One* **2013**, *8*, e73076.
20. von Schillde, M.A.; Hormannsperger, G.; Weiher, M.; Alpert, C.A.; Hahne, H.; Bauerl, C.; van Huynegem, K.; Steidler, L.; Hrncir, T.; Perez-Martinez, G.*, et al.* Lactocepin secreted by lactobacillus exerts anti-inflammatory effects by selectively degrading proinflammatory chemokines. *Cell Host Microbe* **2012**, *11*, 387-396.
21. Weichhart, T.; Haidinger, M.; Hörl, W.H.; Säemann, M.D. Current concepts of molecular defence mechanisms operative during urinary tract infection. *European Journal of Clinical Investigation* **2008**, *38*, 29-38.

22. Lominadze, G.; Powell, D.W.; Luerman, G.C.; Link, A.J.; Ward, R.A.; McLeish, K.R. Proteomic analysis of human neutrophil granules. *Molecular & Cellular Proteomics* **2005**, *4*, 1503-1521.
23. Moll, R.; Divo, M.; Langbein, L. The human keratins: Biology and pathology. *Histochem Cell Biol* **2008**, *129*, 705-733.
24. Pieper, R.; Gatlin, C.L.; McGrath, A.M.; Makusky, A.J.; Mondal, M.; Seonarain, M.; Field, E.; Schatz, C.R.; Estock, M.A.; Ahmed, N.*, et al.* Characterization of the human urinary proteome: A method for high-resolution display of urinary proteins on two-dimensional electrophoresis gels with a yield of nearly 1400 distinct protein spots. *Proteomics* **2004**, *4*, 1159-1174.
25. Toledo-Arana, A.; Valle, J.; Solano, C.; Arrizubieta, M.J.; Cucarella, C.; Lamata, M.; Amorena, B.; Leiva, J.; Penades, J.R.; Lasa, I. The enterococcal surface protein, esp, is involved in enterococcus faecalis biofilm formation. *Appl Environ Microbiol* **2001**, *67*, 4538-4545.
26. Muenchhoff, J.; Siddiqui, K.S.; Poljak, A.; Raftery, M.J.; Barrow, K.D.; Neilan, B.A. A novel prokaryotic l-arginine:Glycine amidinotransferase is involved in cylindrospermopsin biosynthesis. *FEBS J* **2010**, *277*, 3844-3860.
27. Tschudin-Sutter, S.; Frei, R.; Weisser, M.; Goldenberger, D.; Widmer, A.F. Actinobaculum schaalii - invasive pathogen or innocent bystander? A retrospective observational study. *BMC Infect Dis* **2011**, *11*, 289.
28. Cecile Le Brun, S.R., Colas Tanchoux, Franck Bruyere, Philippe Lanotte. Urinary tract infection caused by actinobaculum schaalii: A urosepsis pathogen that should not be underestimated. *JMM Case Reports* **2015**.
29. Sturm, P.D.; Van Eijk, J.; Veltman, S.; Meuleman, E.; Schulin, T. Urosepsis with actinobaculum schaalii and aerococcus urinae. *Journal of clinical microbiology* **2006**, *44*, 652-654.
30. Bank, S.; Jensen, A.; Hansen, T.M.; Soby, K.M.; Prag, J. Actinobaculum schaalii, a common uropathogen in elderly patients, denmark. *Emerg Infect Dis* **2010**, *16*, 76-80.
31. Prigent, G.; Perillaud, C.; Amara, M.; Coutard, A.; Blanc, C.; Pangon, B. Actinobaculum schaalii: A truly emerging pathogen?: Actinobaculum schaalii: Un pathogene reellement emergent? *New Microbes New Infect* **2016**, *11*, 8-16.
32. Haraoka, M.; Hang, L.; Frendeus, B.; Godaly, G.; Burdick, M.; Strieter, R.; Svanborg, C. Neutrophil recruitment and resistance to urinary tract infection. *The Journal of infectious diseases* **1999**, *180*, 1220-1229.
33. Flores-Mireles, A.L.; Walker, J.N.; Caparon, M.; Hultgren, S.J. Urinary tract infections: Epidemiology, mechanisms of infection and treatment options. *Nature Reviews Microbiology* **2015**, *13*, 269-284.
34. Springall, T.; Sheerin, N.S.; Abe, K.; Holers, V.M.; Wan, H.; Sacks, S.H. Epithelial secretion of c3 promotes colonization of the upper urinary tract by escherichia coli. *Nat Med* **2001**, *7*, 801-806.
35. Hooton, T.M.; Bradley, S.F.; Cardenas, D.D.; Colgan, R.; Geerlings, S.E.; Rice, J.C.; Saint, S.; Schaeffer, A.J.; Tambayh, P.A.; Tenke, P.*, et al.* Diagnosis, prevention, and treatment of catheter-associated urinary tract infection in adults: 2009 international clinical practice guidelines from the infectious diseases society of america. *Clinical infectious diseases : an official publication of the Infectious Diseases Society of America* **2010**, *50*, 625-663.
36. Foster, T.J.; Geoghegan, J.A.; Ganesh, V.K.; Hook, M. Adhesion, invasion and evasion: The many functions of the surface proteins of staphylococcus aureus. *Nat Rev Microbiol* **2014**, *12*, 49-62.
37. Hendrickx, A.P.; Willems, R.J.; Bonten, M.J.; van Schaik, W. Lpxtg surface proteins of enterococci. *Trends Microbiol* **2009**, *17*, 423-430.
38. Cabanes, D.; Dehoux, P.; Dussurget, O.; Frangeul, L.; Cossart, P. Surface proteins and the pathogenic potential of listeria monocytogenes. *Trends Microbiol* **2002**, *10*, 238-245.
39. Liu, M.; Guo, S.; Hibbert, J.M.; Jain, V.; Singh, N.; Wilson, N.O.; Stiles, J.K. Cxcl10/ip-10 in infectious diseases pathogenesis and potential therapeutic implications. *Cytokine Growth Factor Rev* **2011**, *22*, 121-130.
40. Holden, V.I.; Bachman, M.A. Diverging roles of bacterial siderophores during infection. *Metallomics* **2015**, *7*, 986-995.
41. Moriarity, J.L.; Hurt, K.J.; Resnick, A.C.; Storm, P.B.; Laroy, W.; Schnaar, R.L.; Snyder, S.H. Udp-glucuronate decarboxylase, a key enzyme in proteoglycan synthesis: Cloning, characterization, and localization. *J Biol Chem* **2002**, *277*, 16968-16975.

42. Alteri, C.J.; Smith, S.N.; Mobley, H.L. Fitness of escherichia coli during urinary tract infection requires gluconeogenesis and the tca cycle. *PLoS pathogens* **2009**, *5*, e1000448.
43. Arntzen, M.O.; Karlskas, I.L.; Skaugen, M.; Eijsink, V.G.; Mathiesen, G. Proteomic investigation of the response of enterococcus faecalis v583 when cultivated in urine. *PLoS One* **2015**, *10*, e0126694.
44. Alteri, C.J.; Mobley, H.L.T. Metabolism and fitness of urinary tract pathogens. *Microbiol Spectr* **2015**, *3*.

Supplementary Materials

Table S1 (File S1). Metaproteomic database searches and entire genome sequence-derived protein sequence entries (ORFs) from Homo Sapiens and microbial species colonizing the human urogenital tract, bladder catheters and cause urinary tract infections.

Dataset S1 (File S2). LC-MS/MS based proteomic data for five catheter biofilm extracts derived from specimens of two long-term catheterized patients and for one in vitro *Actinobaculum massiliense* cultured isolate.

Figure S1 (File S3). Glycogen degradation and synthesis pathways and dTDP-L-rhamnose synthesis.